Clinical Science (2020) **00** 1–18
https://doi.org/10.1042/CS20191229

Research Article

Maternal high-fat diet induces long-term obesity with sex-dependent metabolic programming of adipocyte differentiation, hypertrophy and dysfunction in the offspring

Thorsten Litzenburger[1,*], Eva-Kristina Huber[1,*], Katharina Dinger[1,2], Rebecca Wilke[1], Christina Vohlen[1,3], Jaco Selle[1], Mazlum Kadah[4], Thorsten Persigehl[4], Carola Heneweer[4], Jörg Dötsch[3] and Miguel A. Alejandre Alcazar[1,2,3]

[1]University of Cologne, Faculty of Medicine and University Hospital Cologne, Translational Experimental Pediatrics, Department of Pediatric and Adolescent Medicine, Germany; [2]University of Cologne, Faculty of Medicine and University Hospital Cologne, Center for Molecular Medicine Cologne (CMMC), Germany; [3]University of Cologne, Faculty of Medicine and University Hospital Cologne, Department of Pediatric and Adolescent Medicine, Germany; [4]University of Cologne, Faculty of Medicine and University Hospital Cologne, Department of Diagnostic and Interventional Radiology, Germany

Correspondence: Miguel A. Alejandre Alcázar (miguel.alejandre-alcazar@uk-koeln.de)

Maternal obesity determines obesity and metabolic diseases in the offspring. The white adipose tissue (WAT) orchestrates metabolic pathways, and its dysfunction contributes to metabolic disorders in a sex-dependent manner. Here, we tested if sex differences influence the molecular mechanisms of metabolic programming of WAT in offspring of obese dams. To this end, maternal obesity was induced with high-fat diet (HFD) and the offspring were studied at an *early phase* [postnatal day 21 (P21)], a late phase (P70) and finally P120. In the *early phase* we found a sex-independent increase in WAT in offspring of obese dams using magnetic resonance imaging (MRI), which was more pronounced in females than males. While the adipocyte size increased in both sexes, the distribution of WAT differed in males and females. As mechanistic hints, we identified an inflammatory response in females and a senescence-associated reduction in the preadipocyte factor DLK in males. In the *late phase*, the obese body composition persisted in both sexes, with a partial reversal in females. Moreover, female offspring recovered completely from both the adipocyte hypertrophy and the inflammatory response. These findings were linked to a dysregulation of lipolytic, adipogenic and stemness-related markers as well as AMPKα and Akt signaling. Finally, the sex-dependent metabolic programming persisted with sex-specific differences in adipocyte size until P120. In conclusion, we do not only provide new insights into the molecular mechanisms of sex-dependent metabolic programming of WAT dysfunction, but also highlight the sex-dependent development of low- and high-grade pathogenic obesity.

Introduction

Childhood overweight and obesity are global epidemic threats with a steadily rising incidence and the risk for chronic health problems later on [1–3]. The increasing prevalence of obesity results in a higher incidence of obese pregnant and lactating women. Accumulating evidence demonstrates an intergenerational cycle of obesity, with children of obese women being more susceptible to early-onset obesity. This concept has been coined as *metabolic programming* [4–6]. Clinical and experimental studies confirm that maternal obesity during a critical window of development determines metabolic programming of organ structure and physiology in the offspring, and induces metabolic disorders beyond infancy [7–10]. For

*These authors contributed equally to this work.

Received: 28 November 2019
Revised: 19 March 2020
Accepted: 01 April 2020

Version of Record published: 00 xx 00

Clinical Science (2020) **00** 1–18
https://doi.org/10.1042/CS20191229

example, offspring of obese dams exhibit marked accumulation of white adipose tissue (WAT), elevated levels of leptin and inflammatory cytokines, insulin resistance and aggravated metabolic response when exposed to obesogenic diet later in life [10–13]. Understanding the molecular mechanisms of adipose dysfunction after maternal obesity may provide novel avenues to prevent long-term sequelae of metabolic programming.

Obesity is characterized by an accumulation and a dysfunction of WAT that results in an elevated secretion of adipocytokines and hormones. This chronic subacute inflammatory state predisposes to higher risk for metabolic pathologies, including diabetes mellitus and cardiovascular diseases [14,15]. The WAT orchestrates various metabolic pathways and contributes to the metabolic syndrome in a sex-dependent manner [16–19]. The progression of obesity-related disease is often inevitable, and intimately linked to adipocyte dysfunction [20]. In general, WAT dysfunction includes inflammation, senescence, insulin resistance, preadipocyte dysfunction and adipocyte hypertrophy [21]. Interestingly, these changes in adipogenic function do not only trigger obesity-related diseases, but are also hallmarks of ageing [22–24]. However, the molecular mechanisms as well as sex differences in adipogenesis during metabolic programming and WAT function remain elusive.

The timing of adipose tissue development determines the window of vulnerability to metabolic programming. The number of adipocytes is primarily determined early in life and is mostly stable through adulthood [25]. Moreover, adipogenesis and adipocyte function are tightly regulated by the concerted interaction of various growth factors and by the microenviroment, including inflammatory cells, matrix, cytokines, hormones and mechanical stress [26,27]. Disruption of these processes by maternal obesity during development can result in WAT dysfunction with adverse auto- and paracrine as well as systemic effects, ultimately promoting metabolic disorders and diseases [25]. Thus, identification of early-onset molecular mechanisms disrupting adipogenesis and determining adipocyte function in a sex-dependent manner in health and disease may define new targets to prevent or reverse WAT dysfunction and attenuate obesity-related pathologies. Here, we present a comprehensive study, in which we investigated adipogenesis, the senescence-associated secretory phenotype (SASP), inflammatory response and the deposition of WAT up to postnatal day 120 (P120). Our data provide evidence of sex-dependent mechanisms in metabolic programming of WAT and most interestingly, a protection of females from long-term adipocyte hypertrophy.

Materials and methods

Animal procedures

All animal procedures for this manuscript were performed in accordance with the German regulations and legal requirements and were authorized by the local government authorities (LANUV; 2012.A424). All mice (C57BL/6N) were placed in a room with $22 \pm 2^{\circ}$C, were exposed to a light/dark cycle of 12 h each and had *ad libitum* access to water and their respective chow. The animal model of metabolic programming was performed as previously described [10]. Virgin female mice (C57BL/6N) from our own colony received a high-fat diet (HFD; modified catalog no. C1057; Altromin, Lage, Germany) or a standard diet (Co; ssniff catalog no. R/M-H, V1534-0) for 8 weeks after weaning (P21). HFD and Co dams were time-mated with standard diet-fed male mice and continued on their respective diets throughout gestation and lactation. At birth, the litter size of all dams was normalized to six for each litter. Water and chow were available *ad libitum*, and food was withdrawn only for experimental reasons. After weaning at P21, the offspring of HFD and Co dams were fed standard diet until P120. Both male and female offspring were studied: Co^{male}, Co^{female}, HFD^{male} and HFD^{female}. The exact number of animals are listed in the figure legends; the animals of each group and time point were obtained from three to four different litters. After killing the mice at P21 and P70, WAT was excised as previously described [28]. In addition, some mice underwent a magnetic resonance imaging (MRI) analysis at P21, P70 or P120. The animal experiments took place in the Laboratory of the the Department of Pediatric and Adolescent Medicine and the Department of Diagnostic and Interventional Radiology, University Hospital Cologne, Cologne, Germany.

MRI-analysis of body composition

A whole body MRI scan was performed to assess total body volume, total fat volume and fat fraction. MRI scans were acquired on a Philips Ingenia 3.0 T system (Philips Healthcare) combined with a commercially available small animal coil (Philips Research Hamburg, Germany) with heating function to preserve body temperature during the examination. All mice underwent inhalational anesthesia with isoflurane (2.0–2.5%) in air during image acquisition. The MR protocol consisted of a 3D mFFE T1-weighted sequence with following parameters: echo time (TE) 3.41 ms, repetition time (TR) 8.13 ms, flip angle 45°, field of view (FOV) = 80 × 32 mm, matrix 256 × 256, slice thickness 0.35 mm, gap 0 mm, acquired voxel size 0.35 × 0.35 mm and reconstructed voxel size 0.17 × 0.17 mm, number of signal averages (NSA) 2 and standard scan time for 183 slices was 2 min. First, the total body volume was quantified

by circling the offspring's body, starting at the cerebellum and ending when both legs were separated from the ilium. Second, the total fat volume was measured by defining signal-intensity thresholds in order to detect the adipose tissue; adipose tissue has a high signal intensity in T1 when compared with other organs. The intestinal area was excluded to avoid false-positive measurements. Finally, the total fat volume was related to the total body volume to determine the fat fraction.

Physiological data of the offspring

The body weight (in grams) was obtained at each time point (P21, P70 and P120). Subsequently, mice were killed and perigonadal (pg), retroperitoneal and subcutaneous WAT were excised and weighed (grams).

Tissue preparation

Perigonadal WAT (pgWAT) was excised for molecular studies at P21 and P70. A fraction of the pgWAT was immediately frozen and stored at −80°C for protein analysis and assessment of gene expression. Another fraction was fixed in 4% paraformaldehyde (PFA) in phosphate-buffered saline, followed by paraffin embedding for quantitative histomorphological studies. Finally, a third fraction was used to assess β-galactosidase-positive cells as an indicator of senescence.

Hematoxylin and Eosin staining

Five-micrometer cross-sections of the PFA-fixed and paraffin-embedded pgWAT were stained with Hematoxylin and Eosin as previously described [29]. The tissue sections were imaged in a magnification of 20× using the slide scanner (Leica SCN400, Germany). The mean linear intercept (MLI) of adipocytes was measured by using the program '*cell∧D'* and a grid pattern of 50 μm × 50 μm (version 5.1, Olympus Europe SE & Co. KG, Hamburg, Germany). Blood vessels and connective tissue were avoided. The MLI was assessed in six to eight random fields of view per pgWAT section; three sections per animal.

Senescence-associated β-galactosidase staining

Senescence-associated β-galactosidase (SA-β-gal) solution was prepared using 1 mg/ml β X-Gal (5-Bromo-4-Chloro-3-indolyl β D-galactopyranoside; #B4252, Sigma–Aldrich, Germany), 5 mmol/l potassium ferrocyanide [potassium hexacyanoferrate(II) trihydrate; #P3289, Sigma–Aldrich, Germany], 5 mmol/l potassium ferricyanide [potassium hexacyanoferrate(III) trihydrate; #244023, Sigma–Aldrich, Germany], 150 mmol/l NaCl, 2 mmol/l $MgCl_2$, 0.01% SDS and 0.02% Nonidet-40 (NP40 Alternative, #492016, Calbiochem, Germany). After that, pgWAT was incubated in β-galactosidase for 2 h at 38°C. Subsequently, the tissue was fixed with Tissue-Tec (Sakura Finetek™; #4583 Sakura; Thermo Fisher Scientific, Germany) and frozen at −80°C. The frozen WAT was sectioned (20 μm) using Research Cryostat Leica CM3050S and counterstained with Nuclear Fast Red (Hoelzel Biotech; #BOS-AR0008, Germany). The number of SA-β-gal positive cells was assessed in two fields of view per pgWAT section; one section per animal.

RNA extraction and reverse transcription polymerase chain reaction

Total RNA was isolated from pgWAT using TRIzol (Thermo Fisher Scientific, Germany), and real time reverse transcription polymerase chain reaction (RT-PCR) was performed at P21 and P70 using the 7500 real-time PCR system (Applied Biosystems, Foster City, CA) as described previously [30]. Gene expression was normalized to Hypoxanthine-guanine phosphoribosyltransferase (HPRT) and β-Actin at P21 and P70, respectively. Primers and Taq-Man probes were designed using Primer Express and are listed in Table 1.

Protein isolation and immunoblotting

Protein isolation of pgWAT, measurement of protein concentration and immunoblots were performed as described previously [29]. The blots were incubated with the following antibodies: monoclonal rabbit anti-phospho Akt (pAkt; Cell Signaling Technology, #4058; 1:1000); monoclonal rabbit anti-Akt (Cell Signaling Technology, #9272; 1:2000); monoclonal rabbit anti-phospho 5′ adenosine monophosphate-activated protein kinase α (pAMPKα; Thr^{172}; Cell Signaling Technology, #2535; 1:1000); monoclonal rabbit anti-AMPKα (Cell Signaling Technology, #2603; 1:1000); polyclonal rabbit anti-Δ like non-canonical notch ligand [DLK; Preadipocyte factor 1 (Pref1); abcam, #ab21682; 1:2000]; monoclonal rabbit anti-phospho p38 mitogen-activated protein kinase (pp38; Thr^{180}/Tyr^{182}; Cell Signaling Technology, #4511; 1:1000) and polyclonal rabbit anti-p38 (Cell Signaling Technology, #9212; 1:1000). Monoclonal mouse anti-β-Actin (Cell Signaling Technology, #3700; 1:4000) served as t loading control. Anti-mouse IgG,

Clinical Science (2020) **00** 1–18
https://doi.org/10.1042/CS20191229

Table 1 List of primers used for real-time RT-PCR; TaqMan and SYBR-Green primers

Gene	Method	Primer	Sequence
Leptin (*Lep*)	Taq	for	5′TCACCAGGATCAATGACATTTCAC′3
		rev	3′AGCCCAGGAATGAAGTCCAA5′
		probe	5′ACGCAGTCGGTATCCGCCAAGC′3
Interleukin 1-β (*Il1*β)	Taq	for	5′TGACAGTGATGAGAATGACCTGTTC′3
		rev	3′GGACAGCCCAGGTCAAAGG′5
		taq	ACCCCAAAAGATGAAGGGCTGCTTCC
Metalloproteinase12 (*Mmp12*)	Taq	for	5′GCAGCAGTTCTTTGGGCTAGA′3
		rev	3′GTACATCGGGCACTCCACATC′5
		taq	5′CTGGGCAACTGGACAACTCAACTCTGG′3
Cyclin-dependent kinase inhibitor 1b (*Cdkn1b*)	Taq	for	5′GGAGCAGTGTCCAGGGATGA′3
		rev	3′GGGCGTCTGCTCCACAGT′5
		taq	5′CTTCTTCGCAAAACAAAAGGGCCAACA′3
Cyclin D1 (*Ccnd1*)	Taq	for	5′CGCCCTCCGTATCTTACTTCAA′3
		rev	3′CTCACAGACCTCCAGCATCCA′5
		taq	5′CCATGCGGAAAATCGTGGCCAC′3
Sirtuin 1 (*Sirt1*)	Taq	for	5′GGCTTGAGGGTAATCAATACCTGTT′3
		rev	3′GCATGTGCCACTGTCACTGTT′5
		taq	5′ATGACGTCTTGTCCTCTAGTTCCTGTGGCA′3
Catenin β 1 (*Ctnnb1*)	Taq	for	5′GGACGTTCACAACCGGATTG′3
		rev	3′GGACCCCTGCAGCTACTCTTT′5
		taq	5′CCATTGTTTGTGCAGTTGCTTTATTCTCCC′3
Krüppel-like factor 4 (*Klf4*)	Taq	for	5′CAGACCAGATGCAGTCACAAGTC′3
		rev	3′ACGACCTTCTTCCCCTCTTTG′5
		taq	5′CTCTCTCCATTATCAAGAGCTCATGCCACC′3
Sterol regulatory element binding transcription factor 1 (*Srebp1*α)	Taq	for	5′CATCGACTACATCCGCTTCTTG′3
		rev	3′GTGATTTGCTTTTGTGTGCACTTC′5
		taq	5′CACAGCAACCAGAAGCTCAAGCAGGA′3
Adiponectin (*Adipoq*)	SYBR	for	5′GACAAGGCCGTTCTCTTCAC′3
		rev	3′CCATACACCTGGAGCCAGAC′5
Cyclin-dependent kinase inhibitor 1a (*Cdkn1a*)	SYBR	for	5′GAACATCTCAGGGCCGAAAA′3
		rev	3′CGTGGGCACTTCAGGGTTT′5
Cyclin-dependent kinase inhibitor 1b (*Cdkn1b*)	SYBR	for	5′GGAGCAGTGTCCAGGGATGA′3
		rev	3′GGGCGTCTGCTCCACAGT′5
Cyclin-dependent kinase inhibitor 2a (*Cdkn2a*)	SYBR	for	5′AACTTCGCGGCCAATCC′3
		rev	3′CCGTGATTGCAAAAAAAGCATTA′5
Perilipin 1 (*Plin1*)	SYBR	for	5′AGGGTGTTACGGATAACGTGGTA′3
		rev	3′GGGTTATCGATGTCTCGGAATTC′5
Perilipin 2 (*Plin2*)	SYBR	for	5′GTCTCGTGGGTGGAGTGGAA′3
		rev	3′CGTGACTCGATGTGCTCAACA′5
Monoacylglycerol lipase (*Mgll*)	SYBR	for	5′TCAATGCAGACGGACAGTACCT′3
		rev	3′CAGCTCCATGGGACACAAAGA′5
Fatty acid-binding protein 4 (*Fabbp4*)	SYBR	for	5′AAGTGGGAGTGGGCTTTGC′3
		rev	3′GACCGGATGGTGACCAAATC′5

HRP-linked (Cell Signaling Technology, #7076, 1:5000) and anti-rabbit IgG, HRP-linked (Cell Signaling Technology, #7074, 1:2000 or 1:1000) were used as secondary antibodies.

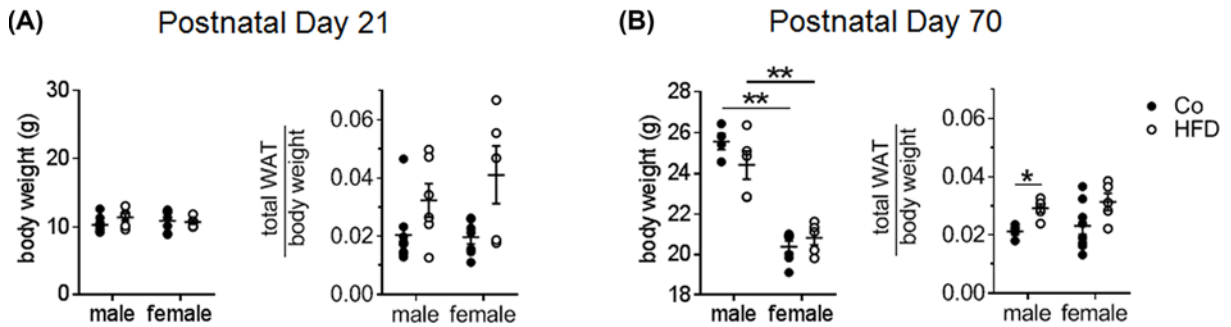

Figure 1. Measurement of body weight and relative WAT in the offspring of obese HFD-fed and control (standard diet-fed, Co) dams at P21 and P70

(**A**) Body weight and total WAT (g) relative to body weight in male and female offspring at P21. (**B**) Body weight and total WAT (g) relative to body weight in male and female offspring at P70. Total WAT includes pg, retroperitoneal and subcutaneous WAT. Co, black bar; HFD, white bar; n=4–10 animals per group; mean ± SEM; *Student's t test and Mann–Whitney test: *P<0.05; **P<0.01.

Analysis of data

The results of real-time RT-PCR were calculated based on the $-\Delta\Delta C_t$ method and expressed as fold induction of mRNA expression compared with the housekeeping gene (1.0-fold induction). Values are shown as means ± standard error of the mean (SEM). Mann–Whitney test or Student's t test were used to test significance at the given time points. A P-value less than 0.05 was considered significant. Densitometric analysis of protein bands was performed using Bio-Rad ImageLab software (Bio-Rad, Munich, Germany). Band intensities from samples were normalized for loading using the β-Actin band from the same sample.

Results

Maternal obesity induces obese body composition with sex-dependent distribution in the offspring

Maternal obesity was induced in virgin female mice by feeding HFD for 8 weeks prior mating; the future control dams (Co) received standard diet. Both groups continued on their respective diets during pregnancy and lactation. The offspring were investigated and divided in four groups: Co^{male}, Co^{female}, HFD^{male} and HFD^{female}. First, we queried if there are sex-dependent differences regarding the impact of maternal obesity on body weight. At P21, both body weight and relative WAT were slightly higher in HFD^{male} when compared with Co^{male}, respectively; in contrast, females did not exhibit differences in body weight, but a mild increase in fat mass after maternal obesity (Figure 1A). At P70, we found the opposing effect: the body weight was rather reduced, whereas the relative WAT was significantly higher in HFD^{male} when compared with Co^{male}. On the contrary, HFD^{female} exhibited a similar body weight like Co^{female} and the relative WAT was not significantly higher (Figure 1B). We next performed MRI studies to measure body volume (ml) and fat fraction (%) in the offspring. Representative MRI images illustrate fat mass and distribution in HFD^{male} and HFD^{female} in comparison with their respective controls Co^{male} and Co^{female} at P21 (Figure 2A) and P70 (Figure 2C). At P21, the body volume was slightly augmented in males after HFD and significantly higher in females. Likewise, the fat fraction was markedly greater in HFD^{male} than Co^{male}; this effect was even more pronounced in HFD^{female} (Figure 2B). At P70, we found no effect of maternal obesity on body volume, but the fat fraction remained significantly higher in males and slightly in females after maternal obesity. However, the fat fraction in females after maternal obesity compared with Co^{female} was less augmented at P70 than at P21, indicating a partial reversal coupled with a physiological increase in WAT in females (Figure 2D). Finally, we studied if the time- and sex-dependent effects of maternal obesity on inflammatory response, differentiation and metabolism of adipose tissue have long-term effects on body composition and adipocyte size in the offspring. Representative MRI images at P120 are shown in Figure 2E. There were no differences in body volume between Co and HFD in males or females. The fat fraction, however, was higher by almost two-fold in HFD^{male} and HFD^{female} when compared with the sex-matched control (Figure 2F).

We next analyzed WAT distribution by measuring the mass of the different compartments after dissection. At P21, we determined a marked increase in retroperitoneal and pgWAT in HFD^{male} when compared with Co^{male}, whereas in females only pgWAT was higher after maternal obesity (Figure 2G). At P70, we observed a shift in WAT distribution in males with a marked increase in subcutaneous WAT in both HFD^{males} and $HFD^{females}$ when compared with Co^{male}

Clinical Science (2020) **00** 1–18
https://doi.org/10.1042/CS20191229

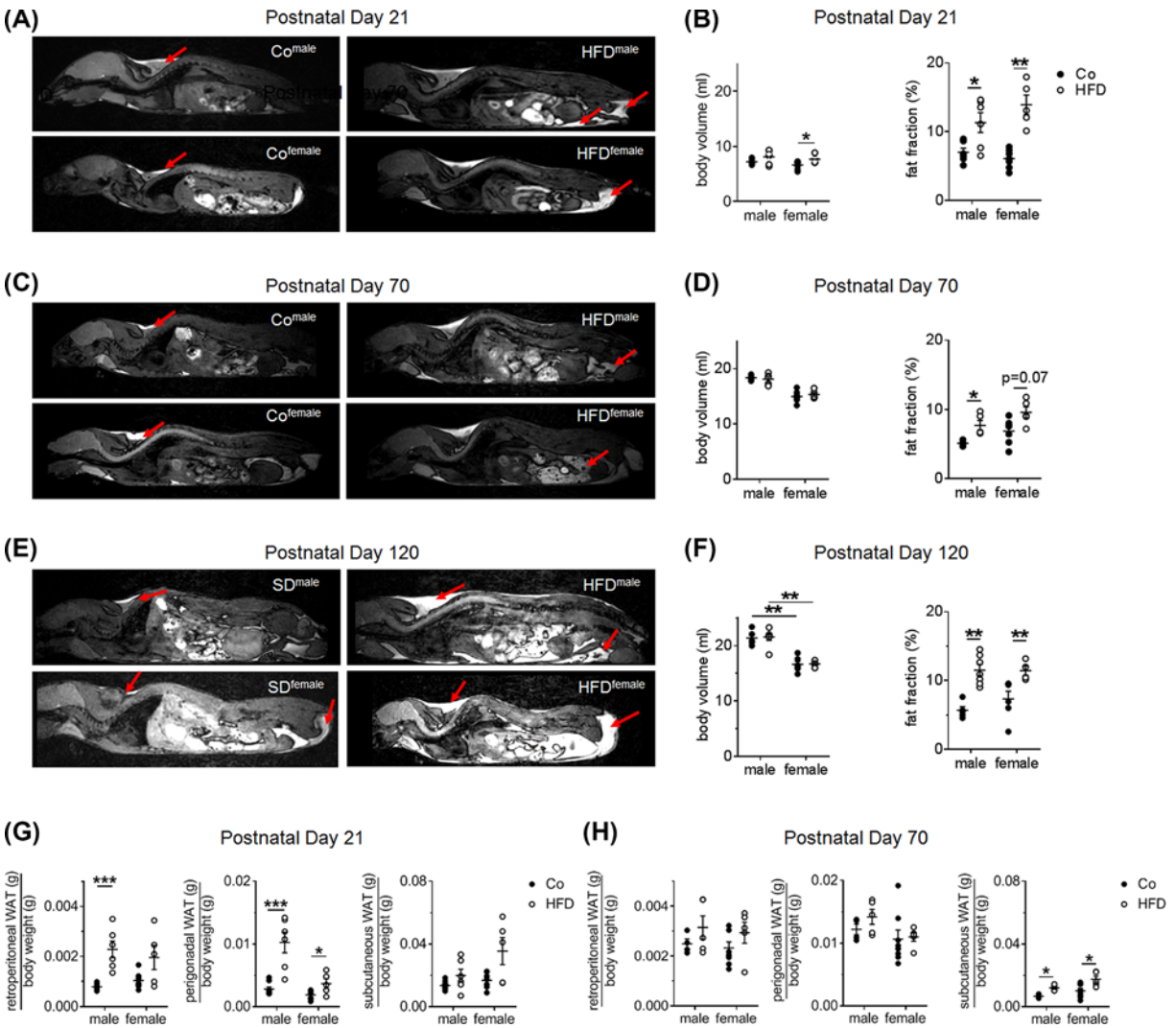

Figure 2. Assessment of body composition and fat distribution

(**A**,**B**) Representative MRI images showing male and female offspring of obese HFD-fed and control (standard diet-fed, Co) dams at P21 (A) Co^{male}, HFD^{male}, Co^{female}, and HFD^{female}; red arrows are depicting fat tissue. Measurement of body volume (ml) and fat fraction (%) are shown next to the MRI images (B). (**C**,**D**) Representative MRI images showing Co^{male}, HFD^{male}, Co^{female} and HFD^{female} at P70 (C); red arrows are depicting fat tissue. The respective body volume (ml) and fat fraction (%) are shown next to the MRI images (D). (**E**,**F**) Assessment of long-term body composition. Representative MRI images showing male and female offspring of obese HFD-fed and control (standard diet-fed, Co) dams at P120: Co^{male}, HFD^{male}, Co^{female} and HFD^{female}; red arrows are depicting fat tissue (E). Measurements of body volume (ml) and fat fraction (%) are shown next to the MRI images (F). (**G**,**H**) Measurement of dissected WAT in different compartments in gram relative to body weight in grams from Co^{male}, HFD^{male}, Co^{female} and HFD^{female} at P21 (G) and P70 (H) retroperitoneal, pg and subcutaneous. Co, black bar; HFD, white bar; n=4–12 animals per group; mean ± SEM; *Mann–Whitney test: $^{*}P<0.05$; $^{**}P<0.01$; $^{***}P<0.001$.

or Co^{female}, respectively (Figure 2H). In conclusion, maternal obesity has a modest impact on body weight in both sexes, but induces a persistent obese body composition with a sex-dependent fat distribution.

Maternal obesity programs adipocyte size in a sex-dependent manner

Having shown that maternal obesity induces an obese body composition and a sex-dependent fat distribution let us study the adipocyte size. Since our previous studies investigated pgWAT and the distribution of pgWAT was markedly different in male and female offspring after maternal obesity in the present study, we performed quantitative histomorphometric analysis using this WAT. Representative H&E-stained images are displayed in Figure 3A (P21), B (P70)

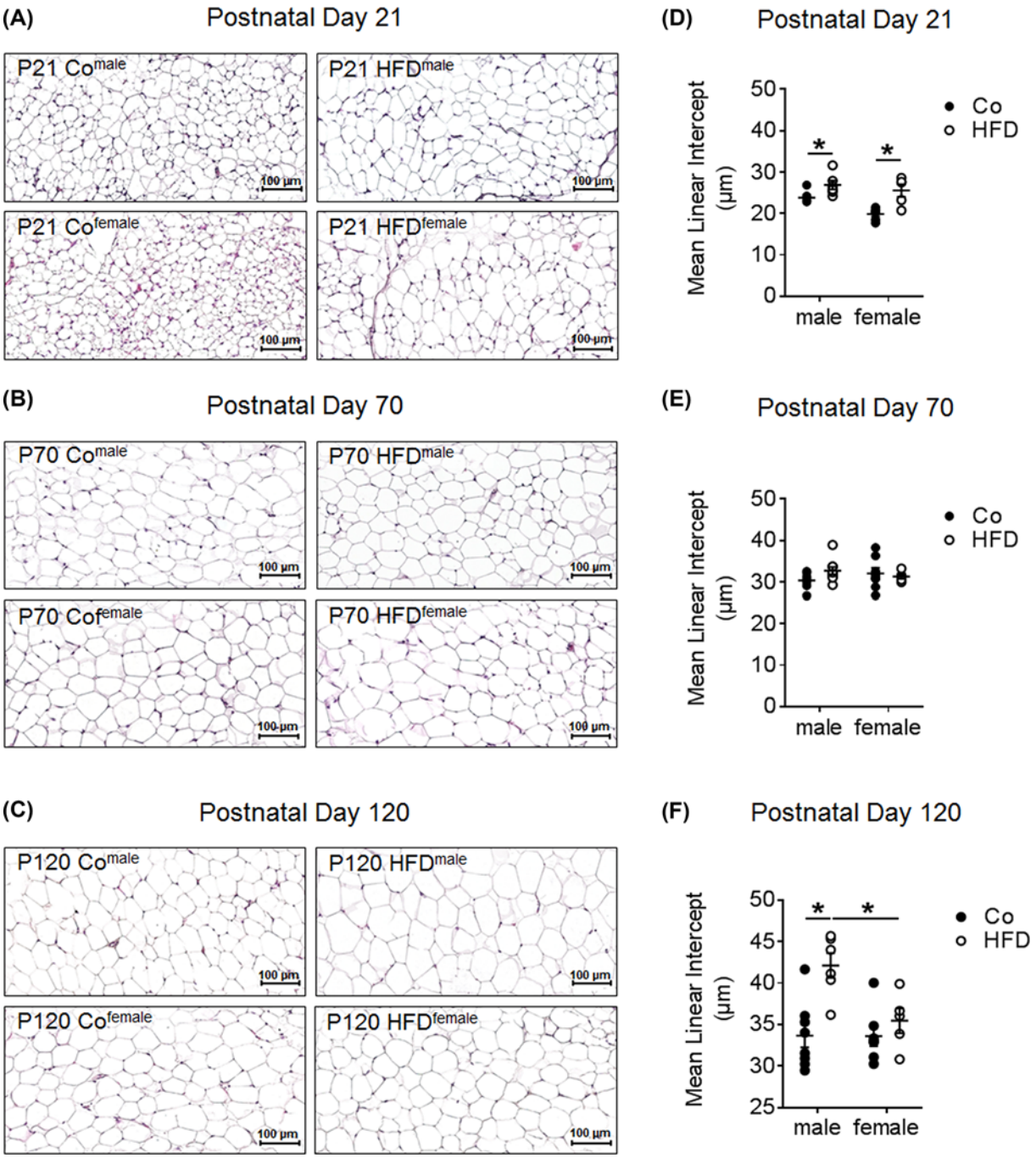

Figure 3. Quantitative histomorphometric analysis of adipocyte size in pgWAT

(**A**–**C**) Representative images of H&E-stained WAT sections from male and female offspring of obese HFD-fed and control (standard diet-fed, Co) dams at P21 (A), P70 (B), and P120 (C) Co^{male}, HFD^{male}, Co^{female}, and HFD^{female}. (**D**–**F**) Assessment of adipocyte size at P21 (D), P70 (E), and P120 (F) using MLI (µm) as an indicator. Co, black bar; HFD, white bar; n=4–9 animals per group; mean ± SEM; *Mann–Whitney test: *P<0.05.

and C (P120). Assessment of MLI as an indicator of adipocyte size showed a significant increase in both HFD^{male} and HFD^{female} when compared with the respective Co group at P21 (Figure 3D). At P70, however, the MLI remained slightly higher in HFD^{male} (P=0.07), but not in HFD^{female} (Figure 3E). Finally, we analyzed the size of adipocytes at P120 and determined a sex-dependent increase in adipocyte size in the offspring after maternal obesity. HFD^{male} exhibited a significant greater MLI when compared with Co^{male}. Adipocyte size of females, however, was not altered by

Clinical Science (2020) **00** 1–18
https://doi.org/10.1042/CS20191229

HFD (Figure 3F). These data demonstrate a persistent effect of maternal obesity on adipocyte size in males, whereas females recover. In summary, the data show a sex-dependent long-term programming effect of maternal obesity with a persistent obese body composition in both female and male offspring, whereas adipocyte hypertrophy only persisted in males.

Sex-dependent metabolic programming of the inflammatory response in pgWAT

Inflammation is a hallmark of adipose tissue dysfunction and metabolic diseases. Hence, we next analyzed the gene expression of inflammatory mediators in pgWAT in the *early* (P21) and *late phase* (P70). *Early phase* (P21): we found a moderate increase in leptin (*Lep*) mRNA in HFD^{male}, but not HFD^{female} compared with Co^{male} and Co^{female}, respectively (Figure 4A). In contrast, adiponectin (*AdipoQ*) mRNA expression was higher in females after maternal obesity, whereas males were not affected (Figure 4B). Interestingly, key inflammatory macrophage markers, such as interleukin 1β (*Il1*β) and metalloproteinase 12 (*Mmp12*), were up-regulated in females after maternal obesity when compared with HFD^{male} (Figure 4C,D). We next assessed the activation of the inflammatory p38 signaling and found a two-fold greater phosphorylation of p38 (pp38) relative to total p38 that was rather reduced in females after maternal obesity than in males (Figure 4E). When p38 was compared with the loading control (β-Actin) we only found a significantly greater activation in SD^{female} than SD^{male}, possible due to interindividual variability.

Late phase (P70): we found a marked sex-dependent reversal of the early inflammatory and metabolic response of pgWAT. The *Lep* expression was not only lower in HFD^{male} when compared with Co^{male}, but also in general lower in females than males. *AdipoQ* mRNA was neither significantly regulated by sex nor by maternal obesity (Figure 4F,G). Regarding inflammatory markers, HFD did not affect the expression of *Il1*β and *Mmp12* in either sex; however, both genes were significantly lower by up to 80% in females when compared with males (Figure 4H,I). While phosphorylated p38 relative to total p38 was not regulated by maternal obesity, it was lower in Co^{female} than in Co^{male} (Figure 4J), suggesting a time- and sex-dependent inflammatory expression pattern in adipose tissue.

Maternal obesity has long-term sex-dependent effects on the cell cycle machinery of adipocytes

The preceding results demonstrate changes in adipocyte size and the inflammatory expression pattern. We next tested, if these changes are related to altered expression of cell cycle-regulating genes in pgWAT. At the *early phase* (P21; Figure 5A–E) we determined no sex- or HFD-dependent effect on gene expression of cyclin-dependent kinase inhibitor 1a (*Cdkn1a*, P21), cyclin-dependent kinase inhibitor 1b (*Cdkn1b*, P27), cyclin D1 (*Ccnd1*) and NAD-dependent deacetylase sirtuin-1 (*Sirt1*); however, gene expression of cyclin-dependent kinase inhibitor 2a (*Cdkn2a*, P16) was regulated by sex with a significant increase in Co^{female} when compared with Co^{male}.

On the contrary, we determined marked regulation of the aforementioned cell cycle regulating genes at the *late phase* (P70, Figure 5F–J): Cell cycle inhibitory markers (*Cdkn1b* and *Cdkn2a, Sirt1*) were significantly reduced in a sex-dependent manner in HFD^{female} compared with Co^{female}. Gene expression of *Cdkn1a* was neither regulated by sex or maternal obesity. However, the proliferative marker *Ccnd1* was significantly up-regulated in HFD^{male} when compared with Co^{male} and not affected in females. In summary, these findings demonstrate a time- and sex-dependent expression of genes encoding for cell cycle-regulating markers, favoring proliferation in females, but less in males after maternal obesity.

Differentiation of adipocytes is time- and sex-dependent after maternal obesity

Preadipocytes are central in adipogenesis and adipose tissue function. They not only serve as progenitors of adipocytes, but they also contribute to adipose tissue dysfunction by adopting inflammatory macrophage-like or senescence-associated phenotype. Therefore, we assessed differentiation markers, such as Perilipin1 and 2 (*Plin1* and *Plin2*) in pgWAT at P21 and P70. At the *early phase* (P21, Figure 6A), we found that both HFD^{female} and Co^{female} express more Plin1 and Plin2 than HFD^{male} and Co^{male}, respectively. Interestingly, maternal obesity reduced *Plin2* mRNA significantly in females, but not males when compared with the sex-matched controls. Similarly, gene expression of Krüppel-like factor 4 (*Klf4*; regulator of cell survival and differentiation) was significantly lower in HFD^{female} than in HFD^{male}. Gene expression of Catenin β 1 (*Ctnnb1*; regulator of stemness) was not regulated by sex or maternal obesity. At the *late phase* (P70, Figure 6C), we found a lower *Plin1* and *Plin2* mRNA after maternal obesity independent of sex. Interestingly, the gene expression of *Klf4* and *Ctnnb1* was significantly lower in HFD^{female} when compared with either Co^{female} or HFD^{male}. To further investigate if the differentiation of preadipocytes is regulated

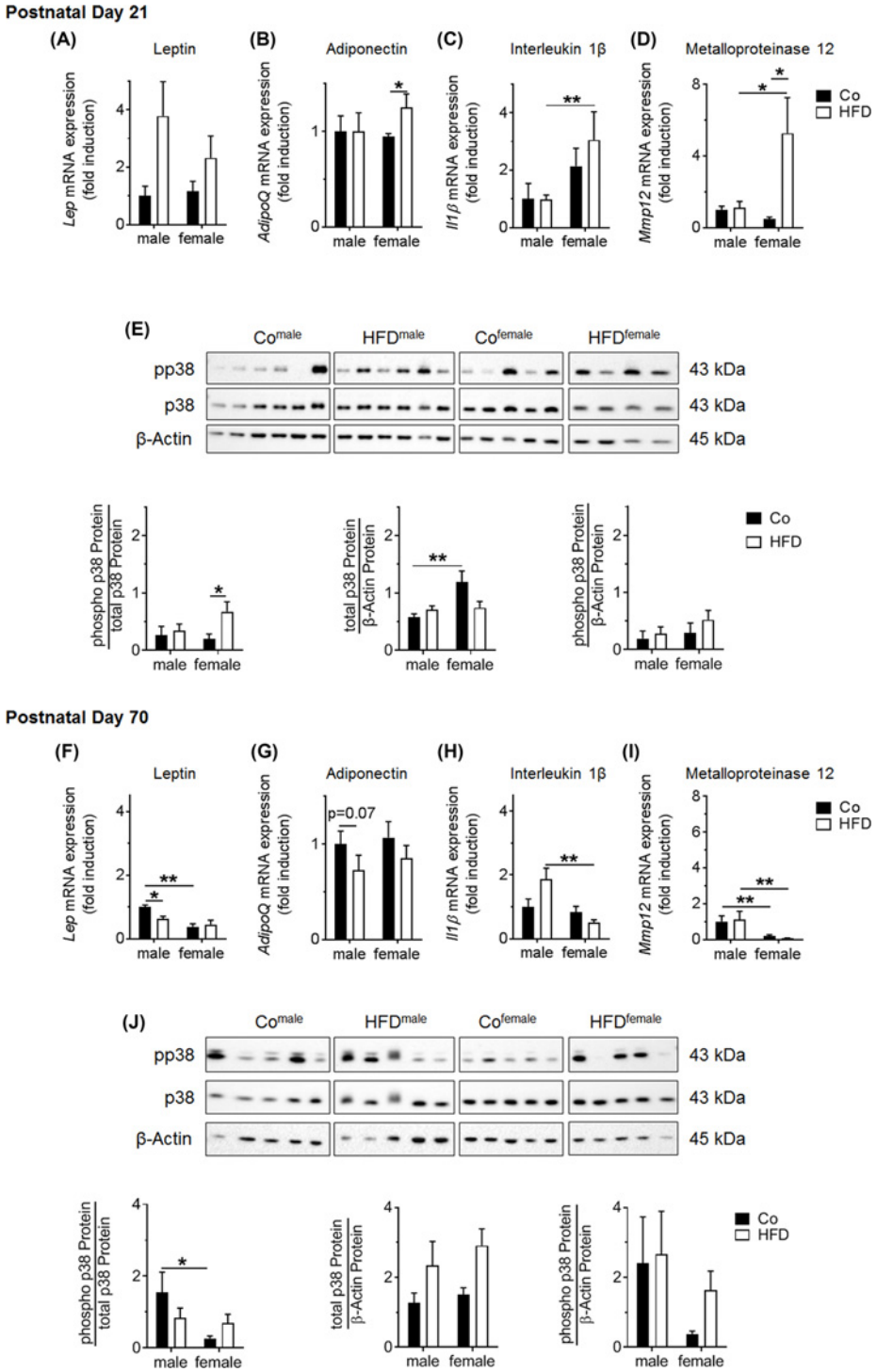

Figure 4.

Assessment of adipokine expression and p38 signaling in pgWAT after maternal obesity at P21(**A**–**E**) and P70 (**F**–**J**). (A–D,F–I) Measurement of gene expression in WAT in male and female offspring of obese HFD-fed and control (standard diet-fed, Co) dams at P21 (A–E) and P70 (F–J) using qRT-PCR: Co^{male}, HFD^{male}, Co^{female} and HFD^{female}. Adipokines: leptin (*Lep*; A,F); adiponectin (*AdipoQ*; B,G); interleukin 1β (*Il1*β; C,H) and metalloproteinase 12 (*Mmp12*; D,I). (E,J) Immunoblot showing phosphorylated p38 (pp38) and total p38 in WAT of Co^{male}, HFD^{male}, Co^{female} and HFD^{female} at P21 (E) and P70 (J); β-Actin served as loading control. The quantitative densitometric summary is shown next to respective immunoblot; pp38 was related to total p38 or β-Actin; total p38 was related to β-Actin. Co, black bar; HFD, white bar; n=4–8 animals per group; mean ± SEM; *Mann–Whitney test: $^{*}P<0.05$; $^{**}P<0.01$.

Clinical Science (2020) **00** 1–18
https://doi.org/10.1042/CS20191229

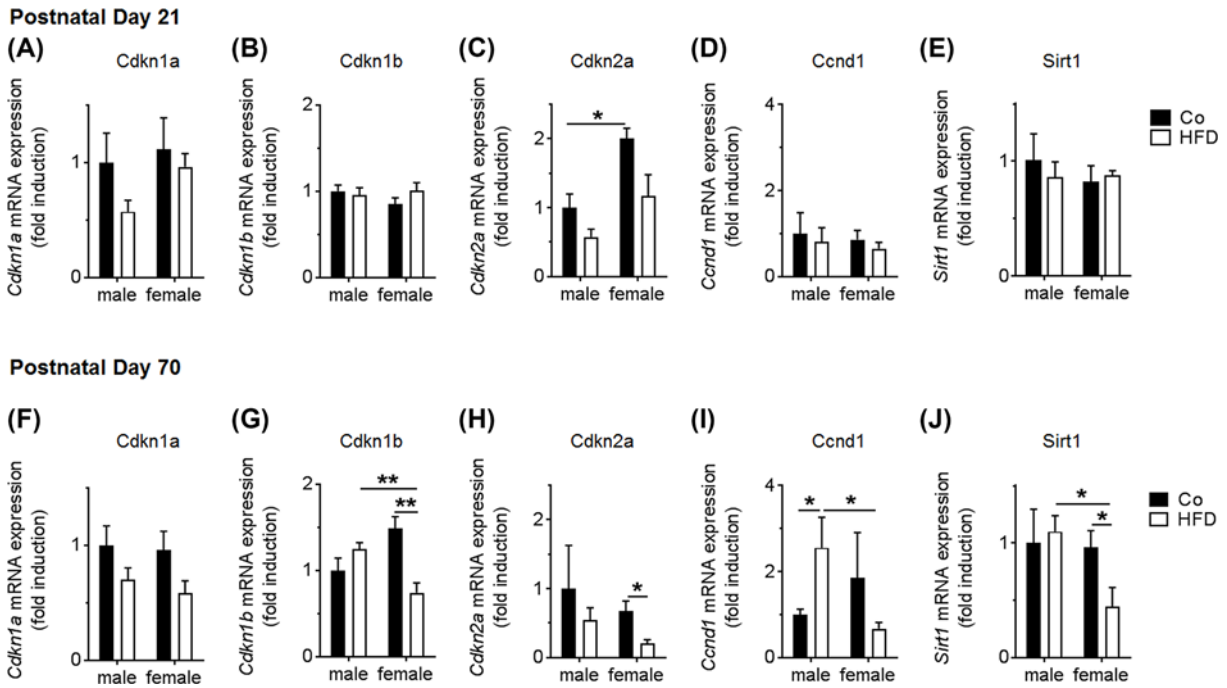

Figure 5.

Assessment of the expression of genes encoding cell cycle regulators in pgWAT from male and female offspring of obese HFD-fed and control (standard diet-fed, Co) dams at P21 (**A**–**E**) and P70 (**F**–**J**) using qRT-PCR: Co^{male}, HFD^{male}, Co^{female} and HFD^{female}. Genes: *Cdkn1a* (p21; A,F); *Cdkn1b* (p27; B,G); *Cdkn2a* (p16; C,H); *Ccnd1* (D,I); NAD-dependent deacetylase *Sirt1* (E,J). Co, black bar; HFD, white bar; n=4–6 animals per group; mean ± SEM; *Mann–Whitney test: $^{*}P<0.05$; $^{**}P<0.01$.

in a sex-specific manner after maternal obesity, we assessed protein abundance of DLK, which inhibits preadipocyte differentiation as well adipogenesis. At P21, but not P70 we found a markedly lower DLK in males, but not females after maternal obesity (Figure 6B,D). In summary, maternal obesity regulates differentiation markers of adipocytes in a time- and sex-specific manner.

Maternal obesity regulates AMPKα and Akt signaling in a sex-dependent manner

Energy metabolism and differentiation of adipocytes are important in the maintenance of adipose tissue function. Since both AMPKα and Akt signaling are central in these processes and regulated by cytokines and hormones, we studied their activation in pgWAT using immunoblots. *Early phase* (P21; Figure 7A,C): first, we assessed phosphorylated AMPKα (pAMPKα) relative to total AMPKα and found lower activation in Co^{female} when compared with Co^{males}. Maternal obesity, however, increased pAMPKα in males significantly and in females slightly (P=0.06). Second, we measured phosphorylated Akt (pAkt) and found sex-dependent differences with a greater activation in HFD^{female} than in HFD^{male}. At the *late phase* (P70; Figure 7B,D) we determined opposing effects: pAMPKα was significantly lower in Co^{female} than in Co^{male}. Maternal obesity only reduced AMPKα signaling in males, but did not have any effect in females. On the other hand, pAkt was greater in HFD^{male} when compared with HFD^{female}. In summary, maternal obesity regulates AMPKα and Akt signaling in a time- and sex-dependent manner. At the early phase, AMPKα and Akt are markedly activated in males and females, respectively; whereas this shifts at the late phase, possibly reflecting a sex-dependent imbalance in adipokines and insulin sensitivity.

Maternal obesity regulates adipocyte metabolism in a sex-dependent manner

To determine if adipocyte metabolism is differently regulated in the long-term in males and females after maternal obesity we assessed gene expression of monoacylglycerol lipase (*Mgll*), sterol regulatory element-binding protein (*Srebp1*) and fatty acid-binding protein 4 (*Fabp4*) in pgWAT at P70. We found that *Mgll* (Figure 8A) and *Fabp4*

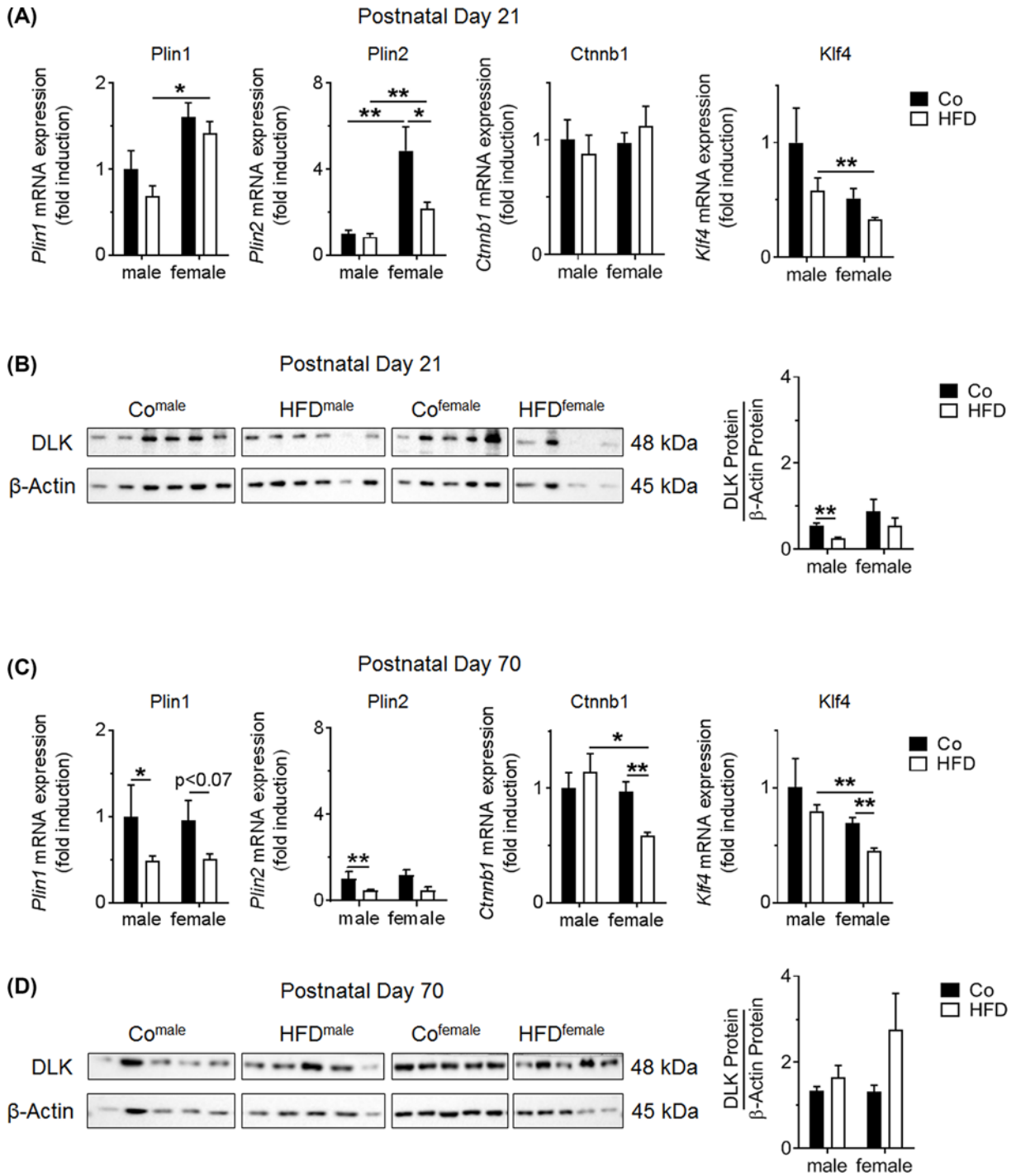

Figure 6.

(**A**,**C**) Measurement of the expression of genes encoding regulators of adipocyte differentiation and stemness in pgWAT from male and female offspring of obese HFD-fed and control (standard diet-fed, Co) dams at P21 (A) and P70 (**C**) using qRT-PCR: Co^{male}, HFD^{male}, Co^{female} and HFD^{female}. Genes: *Plin1*; *Plin2*; *Klf4*; *Ctnnb1*. (**B**,**D**) Immunoblot for DLK (Pref1) as an adipocyte differentiation marker in WAT at P21 (B) and P70 (D); β-Actin served as loading control. The quantitative densitometric summary is shown below to respective immunoblot; DLK was related to β-Actin. Co, black bar; HFD, white bar; n=4–6 animals per group; mean ± SEM; *Mann–Whitney test: $^{*}P<0.05$; $^{**}P<0.01$.

Clinical Science (2020) **00** 1–18
https://doi.org/10.1042/CS20191229

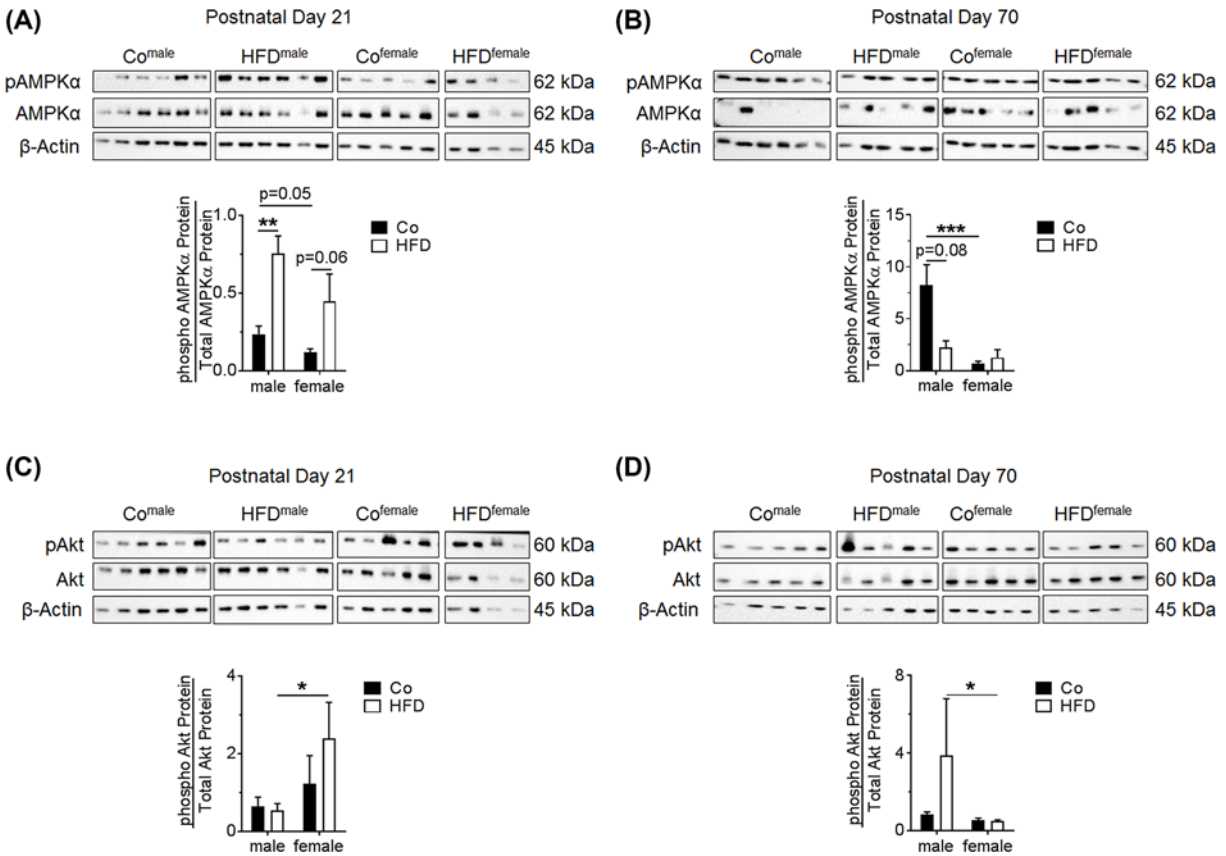

Figure 7.

(**A**,**B**) Immunoblot for pAMPKα and total AMPKα as an indicator of adipokine signaling and regulator of adipocyte homeostasis in pgWAT from male and female offspring of obese HFD-fed and control (standard diet-fed, Co) dams at P21 (A) and P70 (B); β-Actin served as loading control. The quantitative densitometric summary is shown below to respective immunoblot; pAMPKα was related to total AMPKα or β-Actin; total AMPKα was related to β-Actin. (**C**,**D**) Immunoblot for pAkt and total Akt as an indicator of insulin signaling in WAT at P21 (C) and P70 (D); β-Actin served as loading control. The quantitative densitometric summary is shown below to respective immunoblot; pAkt was related to total Akt or β-Actin; total Akt was related to β-Actin. Co, black bar; HFD, white bar; n=4–6 animals per group; mean ± SEM; *Mann–Whitney test: *P<0.05; **P<0.01; ***P<0.001.

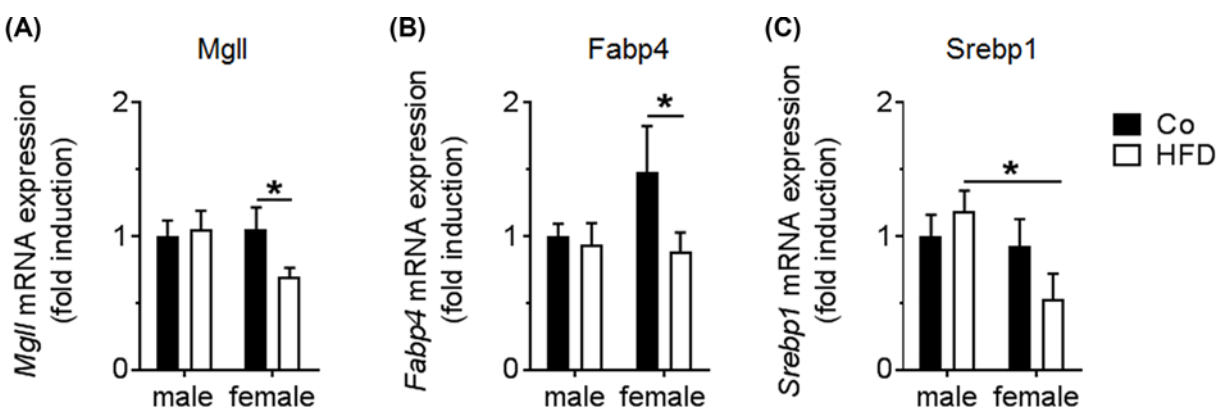

Figure 8. Assessment of expression of genes encoding regulators of adipocyte metabolism in pgWAT from male and female offspring of obese HFD-fed and control (standard diet-fed, Co) dams at P70 using qRT-PCR: Co^{male}, HFD^{male}, Co^{female} and HFD^{female}

Genes: *Mgll* (**A**); *Fabp4* (**B**); *Srebp1* (**C**). Co, black bar; HFD, white bar; n=5–8 animals per group; mean ± SEM; *Mann–Whitney test: *P<0.05.

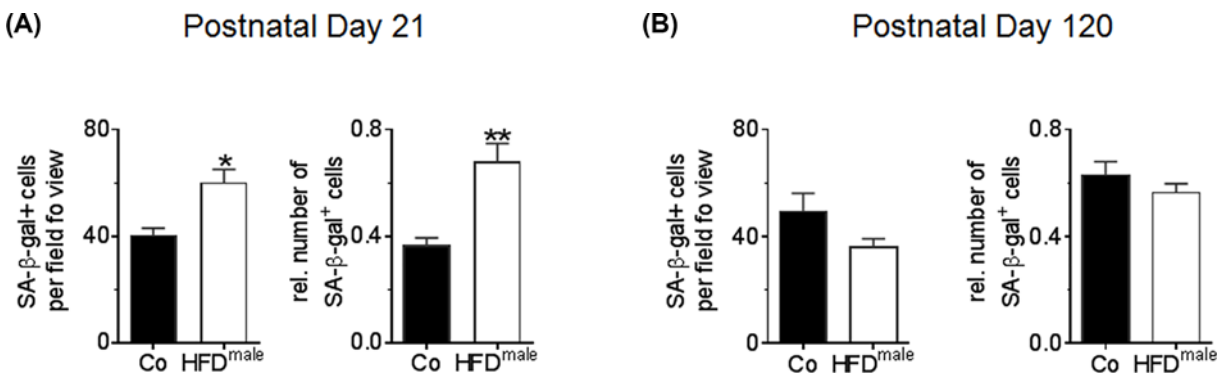

Figure 9.

SA-β-gal staining to assess senescent cells in pgWAT from male offspring of obese HFD-fed (HFD^{male}; black bar) and control (standard diet-fed, Co; white bar) dams at P21 (**A**) and P120 (**B**). The graphs display SA-β-gal positive cells per field of view or the number of SA-β-gal positive cells related to all cells; n=5–8 animals per group; mean ± SEM; *Mann–Whitney test: $^{*}P<0.05$; $^{**}P<0.01$.

(Figure 8B) were significantly lower in HFD^{female} when compared with Co^{female}. This effect was not detected in male offspring after maternal obesity. Moreover, we found that HFD^{female} expressed less *Srebp1* mRNA than HFD^{male} (Figure 8C), confirming a sex-specific programming effect of maternal obesity on adipocyte metabolism.

Maternal obesity induces a transient early senescence in adipocytes of male offspring

Since we found a markedly lower differentiation markers in male offspring after maternal obesity, we next assessed senescence using SA-β-gal staining. We found a higher number of SA-β-gal positive adipocytes per field of view and relative to all cells in pgWAT of male mice at the *early phase* (P21) (Figure 9A). At P120, however, we did not determine any differences in SA-β-gal staining between Co and HFD (similar for females) (Figure 9B).

Discussion

The present study demonstrates two phases of sex-dependent metabolic programming of adipose tissue in offspring of obese dams. First, we identified an *early phase* (P21) after maternal obesity with (i) an obese body composition, which was more pronounced in females than males; (ii) a sex-dependent distribution of the WAT; (iii) a hypertrophy of adipocytes in both sexes; (iv) a greater inflammatory response and leptin expression in females and males, respectively; (v) a sex-dependent activation of AMPKα and Akt pathway; (v) an increase in senescent adipocytes in male offspring.

Second, a *late phase* after maternal obesity was defined by (i) a persistent obese phenotype in both sexes, with a reversal of the hypertrophy of adipocytes and the inflammatory response in females and senescence in males; (iii) sex-dependent pro-proliferative and stemness inhibiting gene expression in females, but not males; (iv) a dysregulation of AMPKα and Akt signaling in WAT from male offspring; (v) a sex-dependent dysregulation of lipid metabolism in pgWAT. Finally, the obese body composition persisted in both females and males, whereas the histological assessment of pgWAT revealed sex-specific differences in adipocyte size.

Sex determines metabolic programming of an obese body composition and fat distribution

Clinical and experimental studies identified maternal obesity as a rising risk factor for the offspring's health and the origin of chronic diseases beyond infancy [5,6,10,31]. A hormonal imbalance coupled with the chronic subacute inflammatory state in obese individuals triggers metabolic disorder, such as insulin resistance and diabetes mellitus [32]. Prior studies confirmed that impaired metabolism and obesity in the offspring after maternal HFD are intimately linked to an inflammatory response. Moreover, we demonstrated higher levels of adipocytokines and hormones of the pgWAT in offspring of obese dams, which then contributed to renal and pulmonary metabolic programming [10,33]. There is accumulating evidence that susceptibility to metabolic disorders is sex-dependent. A significant heterogeneity exists between men and women developing the metabolic syndrome, in large part related to hormonal regulation of

Clinical Science (2020) **00** 1–18
https://doi.org/10.1042/CS20191229

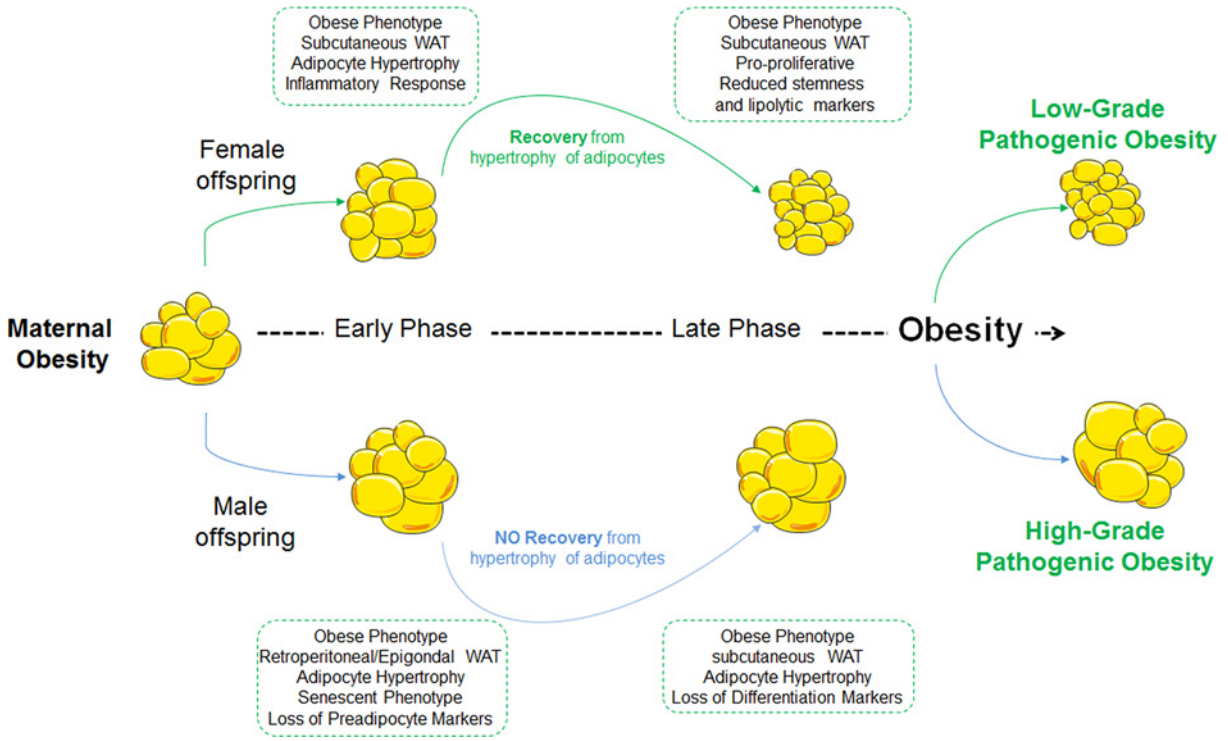

Figure 10. Working model, in which we propose a sex-dependent metabolic programming of adipocyte tissue with an *early phase* (P21) and a *late phase* (P70) in offspring of obese dams

This two-step metabolic programming results in a persistent obese phenotype with sex-specific persistent hypertrophy of adipocytes in males, but not females. Based on these findings we speculate that metabolic programming after maternal obesity favors low-grade pathogenic obesity in females and high-grade pathogenic obesity in males.

body fat distribution and metabolic abnormalities [34–38]. Here, we provide strong evidence that metabolic programming of the WAT is sex-dependent. First, while offspring of both sexes exhibit an obese body composition, obesity was more pronounced in females than males at the *early phase*. Interestingly, this phenotype partially reversed in females at *the later phase*, indicating sex-dependent mechanisms of the adipose tissue. The recovery in females may also be mediated by the reduced expression of antiproliferative cyclin-dependent kinases. Second, the distribution of WAT is not only influenced by gender and age, but also related to aging-related diseases and metabolic syndrome [23,39]. We found marked differences in fat depots at the *early stage* with predominant retroperitoneal and pgWAT in males. Interestingly, the distribution in males shifted to subcutaneous in the *later phase*. These findings suggest a plasticity of the adipose tissue after metabolic programming during the *early phase*.

Sex-dependent metabolic programming of adipocyte size and adipogenic capacity

Whether WAT is a friend or foe is not necessarily defined by its amount, but rather by the localization, the size and the function of adipocytes. For example, hypertrophic adipocytes correlate with systemic insulin resistance, and differ from biochemical functions when compared with smaller adipocytes. These differences involve the expression of anti-inflammatory cytokines, such as adiponectin [40–42]. Prior studies showed that maternal obesity increases adipocyte size and expression of adipokines, including *leptin* and *Il6*, in male offspring [43]. Our present study linked a sex-specific inflammatory response in pgWAT of female offspring after maternal obesity to hypertrophy of adipocytes at the *early stage*; however, this greater adipocyte size was reversed in the *later phase*. In contrast, in males the hypertrophy of adipocytes persisted throughout life. Dysfunction of the adipose tissue has been identified as a hallmark of age-related diseases, including cardiovascular and metabolic disorders as well as cancer. In particular, an inflammatory microenvironment is characteristic of adipose tissue dysfunction in this context. Preadipocytes are not only central in adipogenesis, but also involved in inflammation through a senescent phenotype, characterized

by reduced differentiation and an inflammatory secretome [25]. This has also been coined as a SASP, which is intimately linked to ageing and metabolic disorders [44,45]. Previous studies showed that maternal obesity increased the expression of adipocytokines, e.g. *Il6*, in male offspring, providing initial evidence of an inflammatory phenotype [33,43]. Our present study demonstrates further characteristics of SASP in male mice. For example at the *early stage*, senescence was more pronounced in the adipose tissue of male offspring, which was related to reduced expression of DLK (also known as Pref1), marker of preadipocyte differentiation [46]. Pref1 was originally identified as an inhibitor of adipogenesis and adipocyte differentiation [47]. Pref1 null mice exhibit obesity and elevated adipocyte markers. On the contrary, overexpression of Pref1 decreased adipose mass [48–50]. We speculate that the loss of DLK (Pref1) in male offspring after maternal obesity may trigger the obese phenotype. The reduction in regulators of adipocyte differentiation or stemness, such as Perilipin1 and Perilipin2, in male offspring after maternal obesity was also found during the *late phase* at P70. Both Perilipin1 and Perilipin2 are not only regulators of adipocyte metabolism and lipolysis, but they also regulate differentiation. Loss of these factors affects adipogenesis and triggers inflammation [51–54]. Interestingly, this marked inhibitory effect of maternal obesity on preadipocyte markers was only observed in males, and not in female offspring, suggesting that disruption of adipogenesis by maternal obesity is more effective in males and could account for the long-term sex-dependent changes in size of adipocytes. Since adipocyte size relates to an obese phenotype, our data indicate that metabolic programming may induce low- and high-grade pathogenic obesity in female and male, respectively.

Sex regulates metabolic programming of adipocyte metabolism

Adipocytokines and insulin are crucial in the maintenance of adipocyte homeostasis through AMPKα and Akt signaling pathways, respectively [55,56]. Insulin/Akt promotes the differentiation of preadipocytes to increase the adipose tissue storage capacity [57], and is thereby important in adipogenesis. In contrast, insulin resistance as seen in obese conditions is characteristic for adipose tissue dysfunction [56]. Similarly, AMPK is a key regulator of glucose and energy metabolism as well as stem cell function [55,58]. There is evidence that a lack of AMPKα induces obesity in response to nutrient-overload, identifying thereby AMPKα as a central regulator of adipocytes [55]. In the present study, AMPKα is activated in WAT of male and female offspring during the *early phase*, and contributes to maintenance of differentiation capacity of adipocytes. On the other hand, during the late phase AMPKα signaling was blocked in males, but not females, and thereby may affect adipocyte function and hypertrophy. Moreover, the hypertrophy of adipocytes in male offspring of obese dams compared with females may also be related to a marked activation of Akt signaling in males. Dysregulation of lipolysis and lipogenesis resulting in altered storage of lipids represents another possible explanation for sex-specific hypertrophy of adipocytes. Indeed, key enzymes involved in these processes were regulated in a sex-dependent manner. The expression of monoacylglycerol lipase (*Mgll*), *Srepb1* and *Fabp4* was down-regulated in female mice after maternal obesity when compared with either male offspring of obese dams or control females. Interestingly, *Mgll* null mice fed a HFD gained less body weight than wild-type mice and were protected from insulin resistance and hepatic steatosis [59]. Similarly, SREBP1 promotes hypertrophy of adipocytes and FABP4 is associated with metabolic health [60,61]. Reduced expression of these enzymes may in part explain improved adipocyte function and reversal of early metabolic programming in female offspring.

There are few limitations of the work that need to be discussed and addressed in future studies. Since previous studies from our group investigated pgWAT, we have focused on this compartment of adipose tissue in the present study as well. However, the subcutaneous WAT seems to be markedly affected by perinatal HFD and should be studied in-depth in future studies. Moreover, the question arises wether susceptibility to diet-induced obesity differs between male and female after birth. To this end, a second exposure of adult offspring of obese and lean dams should be performed in the future.

In conclusion, the present study provides a comprehensive analysis of sex-dependent metabolic programming of adipose tissue dysfunction and persistent obese body composition. We do not only demonstrate the long-term impact of maternal obesity on fat fraction and distribution, but we also show two phases of metabolic programming and how sex determines function of the pgWAT. Most intriguingly, female offspring show the capacity to reverse adipocyte hypertrophy and functional changes after the initial metabolic insult by maternal obesity. As depicted in Figure 10, the present study highlights the importance of sex- and gender-dependent differences in the pathogenesis of metabolic diseases, and provides new insights into the molecular mechanisms of sex-dependent metabolic programming of adipose tissue dysfunction, suggesting a low-grade and high grade pathogenic obesity in female and male after maternal obesity, respectively.

Clinical Science (2020) **00** 1–18
https://doi.org/10.1042/CS20191229

Clinical perspectives

- Adipogenesis and adipocyte function are tightly regulated by the microenviroment. Disruption of these processes by maternal obesity can result in metabolic programming of WAT, ultimately promoting obesity-related diseases. Our study aimed to identify molecular mechanisms determining adipocyte function in a sex-dependent manner.
- Maternal obesity induces sex-independent obese body composition and adipose tissue dysfunction in the offspring. While inflammatory signaling is activated in females early in life, the male offspring show early features of SASP and persistent adipocyte hypertrophy. Obesity persists in both sexes up to 3 months. Interestingly, WAT dysfunction and adipocyte hypertrophy reversed in female offspring, but not in male.
- Our data provide new insights into the molecular mechanisms of sex-dependent metabolic programming of WAT dysfunction and possible low- and high-grade pathogenic obesity. This sex-dependent metabolic programming could account for higher clinical susceptibility of males to obesity-related diseases.

Competing Interests

The authors declare that there are no competing interests associated with the manuscript.

Funding

This work was supported by the Deutsche Forschungsgemeinschaft [grant number 1632/2-1 (to M.A.A.A.)]; Marga the und Walter Boll Stiftung [grant number 210-02-16 (to M.A.A.A.)]; the Boehringer Ingelheim Stiftung [grant number XXXX (to M.A.A.A.)]; the Center of Molecular Medicine Cologne (CMMC) [grant number XXXX]; the University Hospital Cologne [grant number XXXX (to M.A.A.A.)]; the Köln Fortune, Faculty of Medicine and University Hospital Cologne, Germany [grant numbers 283/2017 (to K.D. and M.A.A.A.) , 321/2017 (to E.-K.H.)].

Author Contribution

K.D., T.P. and M.A.A.A. conceived and designed the research. T.L., E.-K.H., K.D., R.W., C.V., J.S., M.K., C.H. and M.A.A.A. performed the experiments. T.L., E.K.H., K.D., R.W., J.S., T.P. and M.A.A.A. analyzed the data. T.L., E.K.H., K.D., T.P., C.H., J.D. and M.A.A.A. interpreted the results of experiments. T.L. , E.K.H. and M.A.A.A. prepared the figures. T.L., E.K.H. and M.A.A.A. drafted the manuscript. T.L., E.K.H., K.D., R.W., C.V., J.S., M.K., T.P., C.H., J.D. and M.A.A.A. approved the final version of manuscript. T.L., E.K.H. and M.A.A.A. edited and revised the manuscript.

Acknowledgements

The authors thank the Imaging Facility of Cluster of Excellence for Aging Research (CECAD) at the University of Cologne as well as the support of the Institute of Diagnostic and Interventional Radiology, University Hospital Cologne.

Abbreviations

DLK, Δ like non-canonical notch ligand; HFD, high-fat diet; MLI, mean linear intercept; MRI, magnetic resonance imaging; P, postnatal day; PFA, paraformaldehyde; pg, perigonadal; pgWAT, perigonadal white adipose tissue; pp38, phosphorylation of p38; Pref1, preadipocyte factor 1; RT-PCR, reverse transcription polymerase chain reaction; SASP, senescent-associated secretory phenotype; SA-β-gal, senescence-associated β-galactosidase; WAT, white adipose tissue.

References

1 Ahrens, W. et al. (2014) Prevalence of overweight and obesity in European children below the age of 10. *Int. J. Obes. (Lond.)* **38**, S99–S107, https://doi.org/10.1038/ijo.2014.140
2 Bornhorst, C. et al. (2016) Early life factors and inter-country heterogeneity in BMI growth trajectories of European children: the IDEFICS Study. *PLoS ONE* **11**, e0149268, https://doi.org/10.1371/journal.pone.0149268
3 Ng, M. et al. (2014) Global, regional, and national prevalence of overweight and obesity in children and adults during 1980-2013: a systematic analysis for the Global Burden of Disease Study 2013. *Lancet* **384**, 766–781, https://doi.org/10.1016/S0140-6736(14)60460-8

4 Nicholas, L.M. et al. (2015) The early origins of obesity and insulin resistance: timing, programming and mechanisms. *Int. J. Obes.* **40**, 229, https://doi.org/10.1038/ijo.2015.178
5 Patro Golab, B. et al. (2018) Influence of maternal obesity on the association between common pregnancy complications and risk of childhood obesity: an individual participant data meta-analysis. *Lancet Child Adolesc. Health* **2**, 812–821, https://doi.org/10.1016/S2352-4642(18)30273-6
6 Godfrey, K.M. et al. (2017) Influence of maternal obesity on the long-term health of offspring. *Lancet Diabetes Endocrinol.* **5**, 53–64, https://doi.org/10.1016/S2213-8587(16)30107-3
7 Williams, C.B., Mackenzie, K.C. and Gahagan, S. (2014) The effect of maternal obesity on the offspring. *Clin. Obstet. Gynecol.* **57**, 508–515, https://doi.org/10.1097/GRF.0000000000000043
8 Sutton, E.F. et al. (2016) Developmental programming: state-of-the-science and future directions: summary from a Pennington Biomedical Symposium. *Obesity (Silver Spring)* **24**, 1018–1026, https://doi.org/10.1002/oby.21487
9 Plagemann, A. (2005) Perinatal programming and functional teratogenesis: impact on body weight regulation and obesity. *Physiol. Behav.* **86**, 661–668, https://doi.org/10.1016/j.physbeh.2005.08.065
10 Kasper, P. et al. (2017) Renal metabolic programming is linked to the dynamic regulation of a Leptin-Klf15 axis and Akt/AMPKalpha signaling in male offspring of obese dams. *Endocrinology* **158**, 3399–3415, https://doi.org/10.1210/en.2017-00489
11 Šnajder, D. et al. (2018) Effect of different combination of maternal and postnatal diet on adipose tissue morphology in male rat offspring. *J. Matern. Fetal Neonatal Med.* 1–9
12 Lecoutre, S. and Breton, C. (2015) Maternal nutritional manipulations program adipose tissue dysfunction in offspring. *Front. Physiol.* **6**, https://doi.org/10.3389/fphys.2015.00158
13 Alfaradhi, M.Z. et al. (2016) Maternal obesity in pregnancy developmentally programs adipose tissue inflammation in young, lean male mice offspring. *Endocrinology* **157**, 4246–4256, https://doi.org/10.1210/en.2016-1314
14 Xu, H. et al. (2003) Chronic inflammation in fat plays a crucial role in the development of obesity-related insulin resistance. *J. Clin. Invest.* **112**, 1821–1830, https://doi.org/10.1172/JCI200319451
15 Tilg, H. and Moschen, A.R. (2006) Adipocytokines: mediators linking adipose tissue, inflammation and immunity. *Nat. Rev. Immunol.* **6**, 772–783, https://doi.org/10.1038/nri1937
16 Stubbins, R.E. et al. (2012) Estrogen alters adipocyte biology and protects female mice from adipocyte inflammation and insulin resistance. *Diabetes Obes. Metab.* **14**, 58–66
17 White, U.A. and Tchoukalova, Y.D. (2014) Sex dimorphism and depot differences in adipose tissue function. *Biochim. Biophys. Acta* **1842**, 377–392, https://doi.org/10.1016/j.bbadis.2013.05.006
18 Fuente-Martin, E. et al. (2013) Sex differences in adipose tissue: it is not only a question of quantity and distribution. *Adipocyte* **2**, 128–134, https://doi.org/10.4161/adip.24075
19 Beigh, S.H. and Jain, S. (2012) Prevalence of metabolic syndrome and gender differences. *Bioinformation* **8**, 613–616, https://doi.org/10.6026/97320630008613
20 Gustafson, B. (2010) Adipose tissue, inflammation and atherosclerosis. *J. Atheroscler. Thromb.* **17**, 332–341, https://doi.org/10.5551/jat.3939
21 Klöting, N. and Blüher, M. (2014) Adipocyte dysfunction, inflammation and metabolic syndrome. *Rev. Endocr. Metab. Disord.* **15**, 277–287, https://doi.org/10.1007/s11154-014-9301-0
22 Borengasser, S.J. et al. (2013) Maternal obesity enhances white adipose tissue differentiation and alters genome-scale DNA methylation in male rat offspring. *Endocrinology* **154**, 4113–4125, https://doi.org/10.1210/en.2012-2255
23 Perez, L.M. et al. (2016) 'Adipaging': ageing and obesity share biological hallmarks related to a dysfunctional adipose tissue. *J. Physiol.* **594**, 3187–3207, https://doi.org/10.1113/JP271691
24 Stout, M.B. et al. (2017) Physiological aging: links among adipose tissue dysfunction, diabetes, and frailty. *Physiology* **32**, 9–19, https://doi.org/10.1152/physiol.00012.2016
25 Ghaben, A.L. and Scherer, P.E. (2019) Adipogenesis and metabolic health. *Nat. Rev. Mol. Cell Biol.* **20**, 242–258, https://doi.org/10.1038/s41580-018-0093-z
26 Jeffery, E. et al. (2016) The adipose tissue microenvironment regulates depot-specific adipogenesis in obesity. *Cell Metab.* **24**, 142–150, https://doi.org/10.1016/j.cmet.2016.05.012
27 Pope, B.D. et al. (2016) Microenvironmental control of adipocyte fate and function. *Trends Cell Biol.* **26**, 745–755, https://doi.org/10.1016/j.tcb.2016.05.005
28 Dinger, K. et al. (2016) Early-onset obesity dysregulates pulmonary adipocytokine/insulin signaling and induces asthma-like disease in mice. *Sci. Rep.* **6**, 24168, https://doi.org/10.1038/srep24168
29 Alejandre-Alcázar, M.A. et al. (2007) Hyperoxia modulates TGF-β/BMP signaling in a mouse model of bronchopulmonary dysplasia. *Am. J. Physiol. Lung Cell. Mol. Physiol.* **292**, L537–L549, https://doi.org/10.1152/ajplung.00050.2006
30 Alcazar, M.A.A. et al. (2012) Early postnatal hyperalimentation impairs renal function via SOCS-3 mediated renal postreceptor leptin resistance. *Endocrinology* **153**, 1397–1410, https://doi.org/10.1210/en.2011-1670
31 Heslehurst, N. et al. (2019) The association between maternal body mass index and child obesity: a systematic review and meta-analysis. *PLoS Med.* **16**, e1002817, https://doi.org/10.1371/journal.pmed.1002817
32 Kahn, S.E., Hull, R.L. and Utzschneider, K.M. (2006) Mechanisms linking obesity to insulin resistance and type 2 diabetes. *Nature* **444**, 840–846, https://doi.org/10.1038/nature05482
33 Dinger, K. et al. (2016) Early-onset obesity dysregulates pulmonary adipocytokine/insulin signaling and induces asthma-like disease in mice. *Sci. Rep.* **6**, 24168, https://doi.org/10.1038/srep24168

34 Dearden, L., Bouret, S.G. and Ozanne, S.E. (2018) Sex and gender differences in developmental programming of metabolism. *Mol. Metab.* **15**, 8–19, https://doi.org/10.1016/j.molmet.2018.04.007
35 Arpon, A. et al. (2019) Interaction among sex, aging, and epigenetic processes concerning visceral fat, insulin resistance, and dyslipidaemia. *Front. Endocrinol. (Lausanne)* **10**, 496, https://doi.org/10.3389/fendo.2019.00496
36 Nguyen, L.T. et al. (2017) SIRT1 reduction is associated with sex-specific dysregulation of renal lipid metabolism and stress responses in offspring by maternal high-fat diet. *Sci. Rep.* **7**, 8982, https://doi.org/10.1038/s41598-017-08694-4
37 Chella Krishnan, K., Mehrabian, M. and Lusis, A.J. (2018) Sex differences in metabolism and cardiometabolic disorders. *Curr. Opin Lipidol.* **29**, 404–410, https://doi.org/10.1097/MOL.0000000000000536
38 Pradhan, A.D. (2014) Sex differences in the metabolic syndrome: implications for cardiovascular health in women. *Clin. Chem.* **60**, 44–52, https://doi.org/10.1373/clinchem.2013.202549
39 Jura, M. and Kozak, L.P. (2016) Obesity and related consequences to ageing. *Age (Dordr.)* **38**, 23, https://doi.org/10.1007/s11357-016-9884-3
40 McLaughlin, T. et al. (2007) Enhanced proportion of small adipose cells in insulin-resistant vs insulin-sensitive obese individuals implicates impaired adipogenesis. *Diabetologia* **50**, 1707–1715, https://doi.org/10.1007/s00125-007-0708-y
41 Lundgren, M. et al. (2007) Fat cell enlargement is an independent marker of insulin resistance and 'hyperleptinaemia'. *Diabetologia* **50**, 625–633, https://doi.org/10.1007/s00125-006-0572-1
42 Meyer, L.K. et al. (2013) Adipose tissue depot and cell size dependency of adiponectin synthesis and secretion in human obesity. *Adipocyte* **2**, 217–226, https://doi.org/10.4161/adip.24953
43 Janoschek, R. et al. (2016) Dietary intervention in obese dams protects male offspring from WAT induction of TRPV4, adiposity, and hyperinsulinemia. *Obesity (Silver Spring)* **24**, 1266–1273, https://doi.org/10.1002/oby.21486
44 Xu, M. et al. (2015) Targeting senescent cells enhances adipogenesis and metabolic function in old age. *Elife* **4**, e12997, https://doi.org/10.7554/eLife.12997
45 Newsholme, P. and de Bittencourt, Jr, P.I. (2014) The fat cell senescence hypothesis: a mechanism responsible for abrogating the resolution of inflammation in chronic disease. *Curr. Opin. Clin. Nutr. Metab. Care* **17**, 295–305, https://doi.org/10.1097/MCO.0000000000000077
46 Prestwich, T.C. and Macdougald, O.A. (2007) Wnt/beta-catenin signaling in adipogenesis and metabolism. *Curr. Opin. Cell Biol.* **19**, 612–617, https://doi.org/10.1016/j.ceb.2007.09.014
47 Hudak, C.S. and Sul, H.S. (2013) Pref-1, a gatekeeper of adipogenesis. *Front. Endocrinol. (Lausanne)* **4**, 79, https://doi.org/10.3389/fendo.2013.00079
48 Smas, C.M. and Sul, H.S. (1993) Pref-1, a protein containing EGF-like repeats, inhibits adipocyte differentiation. *Cell* **73**, 725–734, https://doi.org/10.1016/0092-8674(93)90252-L
49 Lee, K. et al. (2003) Inhibition of adipogenesis and development of glucose intolerance by soluble preadipocyte factor-1 (Pref-1). *J. Clin. Invest.* **111**, 453–461, https://doi.org/10.1172/JCI15924
50 Villena, J.A. et al. (2008) Resistance to high-fat diet-induced obesity but exacerbated insulin resistance in mice overexpressing preadipocyte factor-1 (Pref-1): a new model of partial lipodystrophy. *Diabetes* **57**, 3258–3266, https://doi.org/10.2337/db07-1739
51 Takahashi, Y. et al. (2016) Perilipin2 plays a positive role in adipocytes during lipolysis by escaping proteasomal degradation. *Sci. Rep.* **6**, 20975, https://doi.org/10.1038/srep20975
52 McManaman, J.L. et al. (2013) Perilipin-2-null mice are protected against diet-induced obesity, adipose inflammation, and fatty liver disease. *J. Lipid Res.* **54**, 1346–1359, https://doi.org/10.1194/jlr.M035063
53 Sohn, J.H. et al. (2018) Perilipin 1 (Plin1) deficiency promotes inflammatory responses in lean adipose tissue through lipid dysregulation. *J. Biol. Chem.* **293**, 13974–13988, https://doi.org/10.1074/jbc.RA118.003541
54 Lyu, Y. et al. (2015) Defective differentiation of adipose precursor cells from lipodystrophic mice lacking perilipin 1. *PLoS ONE* **10**, e0117536, https://doi.org/10.1371/journal.pone.0117536
55 Wu, L. et al. (2018) AMP-activated protein kinase (AMPK) regulates energy metabolism through modulating thermogenesis in adipose tissue. *Front. Physiol.* **9**, 122, https://doi.org/10.3389/fphys.2018.00122
56 Shimobayashi, M. et al. (2018) Insulin resistance causes inflammation in adipose tissue. *J. Clin. Invest.* **128**, 1538–1550, https://doi.org/10.1172/JCI96139
57 Tomlinson, J.J. et al. (2010) Insulin sensitization of human preadipocytes through glucocorticoid hormone induction of forkhead transcription factors. *Mol. Endocrinol.* **24**, 104–113, https://doi.org/10.1210/me.2009-0091
58 Liu, Y. and Yamashita, J.K. (2019) AMPK activators contribute to maintain naive pluripotency in mouse embryonic stem cells. *Biochem. Biophys Res. Commun.* **509**, 24–31, https://doi.org/10.1016/j.bbrc.2018.11.164
59 Yoshida, K. et al. (2019) Monoacylglycerol lipase deficiency affects diet-induced obesity, fat absorption, and feeding behavior in CB1 cannabinoid receptor-deficient mice. *FASEB J.* **33**, 2484–2497, https://doi.org/10.1096/fj.201801203R
60 Horton, J.D. et al. (2003) Overexpression of sterol regulatory element-binding protein-1a in mouse adipose tissue produces adipocyte hypertrophy, increased fatty acid secretion, and fatty liver. *J. Biol. Chem.* **278**, 36652–36660, https://doi.org/10.1074/jbc.M306540200
61 Prentice, K.J., Saksi, J. and Hotamisligil, G.S. (2019) Adipokine FABP4 integrates energy stores and counterregulatory metabolic responses. *J. Lipid Res.* **60**, 734–740, https://doi.org/10.1194/jlr.S091793